Nuclear Inst. and Methods in Physics Research, A 959 (2020) 163439

Contents lists available at ScienceDirect

Nuclear Inst. and Methods in Physics Research, A

journal homepage: www.elsevier.com/locate/nima

Evaluation of using the Doppler shift effect of prompt gamma for measuring the carbon ion range *in vivo* for heterogeneous phantoms

Changran Geng [a,1], Yang Han [a,c,1], Xiaobin Tang [a,*], Diyun Shu [a], Chunhui Gong [a,b], Saverio Altieri [b,c]

[a] Nanjing University of Aeronautics and Astronautics, Department of Nuclear Science and Technology, 29 Yudao St., Nanjing 210016, China
[b] Istituto Nazionale di Fisica Nucleare (INFN), the section of Pavia, Pavia, Italy
[c] University of Pavia, Department of Physics, Pavia, Italy

ARTICLE INFO

Keywords:
Range verify cation
Prompt gamma spectroscopy
Doppler shift effect
Carbon ion therapy

ABSTRACT

Carbon ion therapy is an advanced radiation treatment modality considering its distinct dose distribution and high biological effectiveness. However, carbon ion therapy has become more sensitive to the range uncertainty comparing to the traditional x-ray radiotherapy because of its steep dose distribution near the Bragg peak, which makes the benefits not been fully utilized. Prompt gamma (PG) spectroscopy is one of the potential choices to achieve the range verification in carbon ion therapy. In this paper, we describe that the Doppler shift effect causes the energy shift of PG (4.44 MeV) produced by the de-excitation of the flying $^{12}C^*$, which makes PG spectroscopy an alternative method for range verification. In order to prove its feasibility of applying this method during patient treatment, Monte Carlo simulation and analytical calculation are compared to verify the accuracy with different materials and non-uniform geometry model. The proposed method is applied to range measurement in the homogeneous phantom filled with different materials (polyethylene, water, and adipose) and the Chinese hybrid radiation phantom with two different irradiated positions (chest and abdomen). Results show that the difference value is less than 2.1% for three homogeneous phantoms. Moreover, good conformance is obtained when using the Chinese hybrid radiation phantom in both irradiated positions. These results prove the feasibility of using the proposed method in a more complicated heterogeneous human model.

1. Introduction

Charged-particle therapy is currently a rapidly developing treatment modality due to its advantages in physical dose distribution, that is, charged particles gradually lose their energy along the beam path and eventually deposit most of their energy at the end of the range [1]. Carbon ion therapy, one kind of charged-particle therapy, has been regarded as the most promising radiation treatment modality considering its extra advantage of high biological effectiveness [2,3]. However, due to the steep dose distribution near the Bragg peak, charged-particle therapy is more sensitive to the range uncertainty comparing to the traditional radiotherapy, which makes the benefits not been fully utilized. The range uncertainty comes from patient positioning, CT resolution, CT conversion factor, biological effect, anatomic change, and beam parameter uncertainty. Hence, the safety margin becomes necessary to prevent under-dosing in the tumor. For instance, the methodology used to generate charged-particle stopping powers from the HU value of CT image is not precisely correct because the conversion requires certain assumptions for the composition and ionization energy of tissues. Various safety margins have been formulated by different cancer treatment centers and organizations to ensure the treatment outcome, for example, 2.5% or 3.5% of the range plus a fixed margin of 1.5 or 3 mm for proton therapy, and 5 mm or 2.5% of the range plus a fixed margin of 2 mm for carbon ion therapy [4,5]. Nevertheless, this manner can be regarded as a compromise such that it increases the normal tissue dose, resulting in a reduced dose advantage of the charged-particle therapy over the conventional therapy. Therefore, developing methodologies for reducing the safety margin has become a hot topic in this field, though the satisfying method for range verification in vivo during the treatment has not been applied in clinical routine.

Most range verification methods during charged-particle therapy rely on the delayed gamma and prompt gamma (PG) emission [6]. Positron emission tomography (PET) has been proposed for range verification by detecting the coincident 511 keV gamma from the annihilation of positrons, which come from the decay of positron-emitting isotopes produced during the charged particle irradiation [7].

* Corresponding author.
E-mail address: tangxiaobin@nuaa.edu.cn (X. Tang).
[1] These authors contributed equally to this work.

https://doi.org/10.1016/j.nima.2020.163439
Received 29 September 2019; Received in revised form 18 December 2019; Accepted 12 January 2020
Available online 15 January 2020
0168-9002/

However, one of the main disadvantages of this method is the washout effect, that is, the location and intensity of the gamma emission do not fully coincide with the location of the nuclear interaction occurring due to biological and physical washout. In-beam or in-room PET can potentially reduce the significance of the washout effect, but the related technical difficulty remains [8,9]. PG detection during charged-particle treatment has gained interest in range verification because of its instantaneity [10,11]. PG comes from the de-excitation of the excited nucleus produced in the nuclear interactions with a time scale shorter than any biological process. Various PG detection methods and systems have been proposed for range verification [12]. Some relative PG detection systems (e.g., slit collimator detection system, array-type detection system, Compton camera) have been developed. However, these methods have to establish the array-type collimator, detection crystal, amplifier, or circuit, which make them expensive. Moreover, numerous difficulties still need to be solved to achieve accurate range verification. An absolute detection method has been proposed for proton range verification based on spectroscopy with PG spectrum detection and the time-of-flight technique [13,14]. However, this method, based on the counts of characteristic PG peaks and gamma emission cross-section, may be difficult to be applied in carbon range verification because of the influence of multiple nuclear fragments, which make the fitting function too complicated according to our preliminary study. Range verification methods by ultrasound have also been developed in recent years [15], but the accuracy remains uncertain.

In this paper, we use the method for carbon ion range verification based on the Doppler shift effect of PG, which was recently proposed by our group [16]. This method is based on PG spectroscopy, but we focus on the characteristics of the PG peak energy rather than the peak count, which has been used during proton therapy with very exciting results. The reason we cannot use the peak count in carbon therapy is that multiple interactions can occur during the carbon beam irradiation, which produces various secondary ion particles making the source of each characteristic PG rather complex. The principle of using doppler effect of PG has been verified using a simplified model in our previous work. The primary carbon ions are possibly excited when they interact with light elements, such as hydrogen, thus releasing characteristic gamma on-the-fly on a short time scale. Considering the well-known relativistic Doppler effect [17], the energy of the emitted gamma (e.g., 4.44 MeV) from $^{12}C^*$ can be shifted to another energy when $^{12}C^*$ is moving at high speed. This phenomenon indicates that the energy-shifted gamma is emitted in a reference system, which moves with the speed of the center of the mass coordinate system (see Fig. 1). Other shifted gamma emitted from other projectiles on-the-fly (i.e., secondary charged particles) may be available. However, it is difficult to be detected or distinguished in the gamma energy spectrum considering its low yield [18]. Given that the shifted energy of this kind of gamma is related to the particle velocity (i.e., the speed of the coordinate system), this physical mechanism allows the prediction of carbon ion energy via the energy spectrum. Then, in vivo range verification can be realized with the knowledge of carbon energy in the detection site.

However, considering the complicated material composition and geometry of the human body, it is necessary to illustrate its feasibility using a more realistic model. The performance of this method in the homogeneous phantoms with different material filled in and inhomogeneous phantoms (i.e., the Chinese hybrid radiation phantom) will be elucidated by comparing the shifted PG energy along the beam path using Monte Carlo method as well as analytical calculation.

2. Methods

2.1. Monte Carlo simulation

2.1.1. Software and physics lists

The Monte Carlo simulation software TOPAS 3.1.2 [19], a particle therapy research-oriented Monte Carlo platform based on Geant4.10.3.p01 [20–22], was used to simulate the multiparticle transport during the carbon ion treatment. The physical model used in this research involved "g4em-standard_opt4", "g4h-phy_QGSP_BIC_HP", "g4decay", "g4ion-binarycascade", "g4h-elastic_HP" and "g4stopping" [16].

2.1.2. Geometric setup and beam configuration

We use the homogeneous phantom with different materials and inhomogeneous voxelated phantom with different fields to perform the carbon beam irradiation in the Monte Carlo simulation (Fig. 2). The size of the cylindrical homogeneous phantom is Ø10 cm × 20 cm filled with polyethylene/water/adipose as the material. A cylindrical air volume (Ø20 cm × 20 cm) surrounds the irradiated phantom. This homogeneous geometry model is similar to that established by Zarifi et al. [23]. We detect the PG spectrum using two phase-spaces, which are used to record the information of particles in a sensitive volume or surface, including its position, direction, energy, and time-of-fight. In phase-space 1, gamma generated in the inner cylinder phantom is recorded. Notably, the secondary gamma is not recorded in this phase-space to reflect the condition of PG generation without the influence of gamma scattering and other interactions. In phase-space 2 (i.e. surface of the outer cylinder volume), all the gamma across the cylindrical surfaces (Ø20 cm) are recorded. Similar to the real treatment, we use the Chinese hybrid radiation phantom (CHRP) of 30-year old male to mimic the patient (Fig. 2b) [24]. This phantom is segmented to $300\times300\times300$ voxels (i.e., $0.567\times0.567\times0.567$ cm^3 for each voxel) for Monte Carlo simulation. The composition of each material refers to the ICRU report 46 [25]. The detect method is the same with phase-space 1.

The carbon ion beam is a pencil beam with 2.9724 mm of Gaussian position broadening, 1mrad Gaussian angle distribution, 200 MeV/u of the energy, and 0.5% of the energy spread. For the homogeneous phantom simulation, the carbon beam is injected in the phantom along the central axis of the cylinder phantom. For the CHRP case, the carbon beam injects to liver in the 90th layer (i.e., 51.03 cm from the overhead) and lung in the 70th layer (i.e., 39.59 cm from the overhead). 5×10^8 carbon ions are used in the simulation to make the statistical error below 2%.

2.2. Analytical calculation

The theoretical relationship between the energy shift and the carbon energy along the beam path can be solved by analytical calculation [16]. According to the relativistic Doppler formula, the frequency of the electromagnetic wave in a specific observing direction can be expressed as follows:

$$f' = f \times \frac{\sqrt{1-\beta^2}}{1-\beta\times\cos\theta}, \tag{1}$$

where f' is the frequency of the electromagnetic wave with the Doppler shift in the observing direction, f is the original frequency of the electromagnetic wave, β is the ratio of speed between carbon ions to the light in vacuum, and θ is the detected direction, which is the angle between the detection line and the moving direction of the carbon beam.

Given $E_\gamma = \hbar f$, we know

$$E'_\gamma = E_\gamma \times \frac{\frac{m_0c^2}{m_0c^2+E_c}}{1-\cos\theta\times\sqrt{1-\left(\frac{m_0c^2}{m_0c^2+E_c}\right)^2}}, \tag{2}$$

which represents the relationship between shifted gamma energy (E'_γ) and carbon energy (E_c) [16]. The shifted gamma energy is a function of depth as the carbon ion energy along the beam path can be solved numerically by the famous Bethe–Bloch formula.

We get the difference value (S_i) by comparing the results of the shifted PG energy at different depths (i) along the beam path via Monte

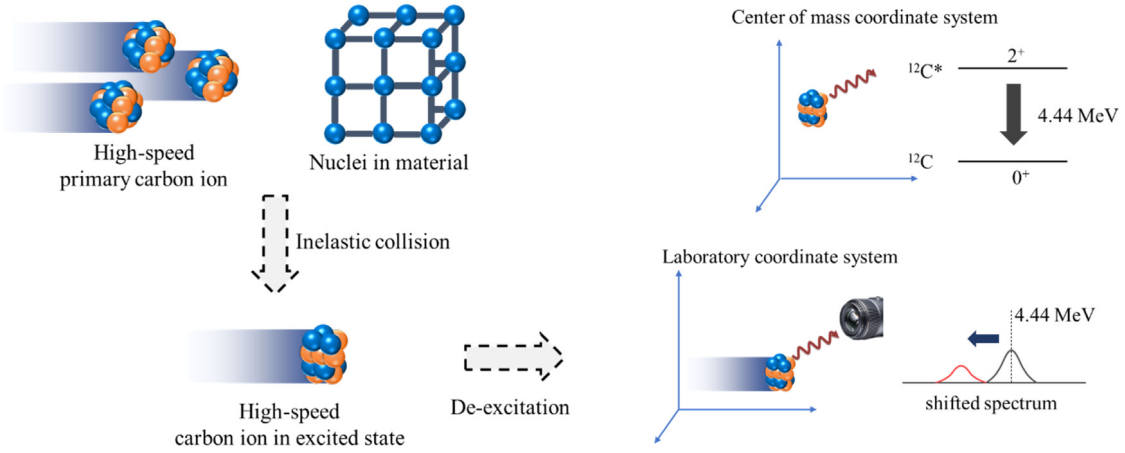

Fig. 1. Schematic of the shifted PG generated in carbon ion therapy.

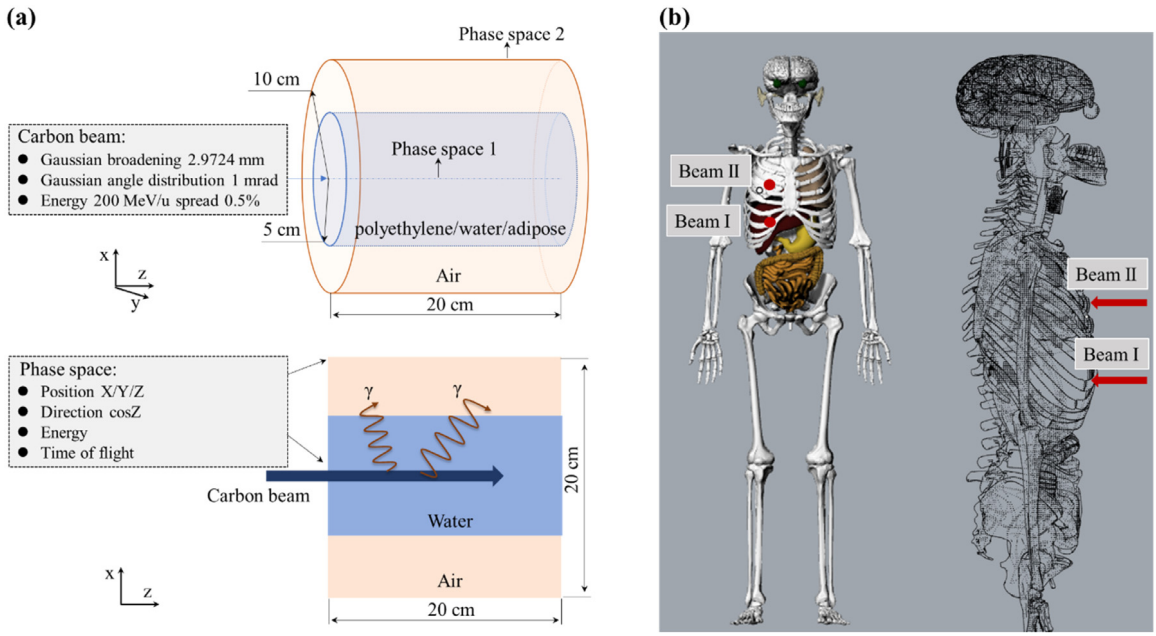

Fig. 2. Schematics of (a) the homogeneous phantom and (b) the Chinese hybrid radiation phantom in the simulation.

Carlo simulation (E_i^{ana}) and analytical calculation (E_i^{mc}) to evaluate the feasibility and accuracy of the proposed method as follows:

$$S_i = \frac{E_i^{ana} - E_i^{mc}}{E_i^{ana}} \times 100\%. \quad (3)$$

3. Results and discussion

3.1. PG energy spectra in the homogeneous phantom

In our previous work, we have done some simulation using the detector system with a physical slit collimator [16]. However, it could be inefficient when it comes to a much more complicated phantom like we showed in Fig. 2b. To reduce the calculation time, we need to find a replaceable method. For such a purpose, a comparison between spectra using different data scored method (i.e., phase-space I and II with different angle limitations) is shown in this section. PG energy spectra measured using the polyethylene phantom by the Monte Carlo simulation are shown in Figs. 3, 4, and 5. In these spectra, there are significant characteristic PG peaks. However, compared to the case with water phantom, PG peaks with the energy of 5.27 and 6.18 MeV disappear. On the other hand, the shifted PG peak, which we should concentrate on, shows a similar trend with the literature. Fig. 3 shows the PG spectra detected in phase-space I at the depth of 6, 6.9, 7.8, 8.8, and 9.2 cm with the emission direction with respect to Z-axis restricted from 85 to 95 degrees, which is used to simulate the collimator system considering most of the collimator is perpendicular to the beam path. The result indicates the presence of the characteristic PG peak with the energy of 4.44 MeV in each curve of Fig. 3. This PG peak comes from the excited ^{12}C with low kinetic energy produced during the nuclear collision considering its characteristic nuclear energy level. In Figs. 3a, 3b and 3c, a significant PG peak with the energy less than 4.44 MeV is observed, and its position is different in the two figures. We called it red-shifted peak, which is shifted from the 4.44 MeV PG peak caused by the Doppler shift effect. The energy of the shifted PG peak in the Figs. 3a, 3b and 3c is different because in the different depths of the beam path, the energy of the flying carbon ions which is the primary source of these shifted PG is different, and also according to the Formula 2, there should be different shifted PG energy with different carbon ion energy. In Fig. 3d, because of the peak overlap, the shifted PG peak and 4.44 MeV characteristic peak cannot be distinguished easily. In Figs. 3e and 3f, there is no shifted PG peak which also proves the hypothesis because the range of the 200 MeV/u carbon ion in the

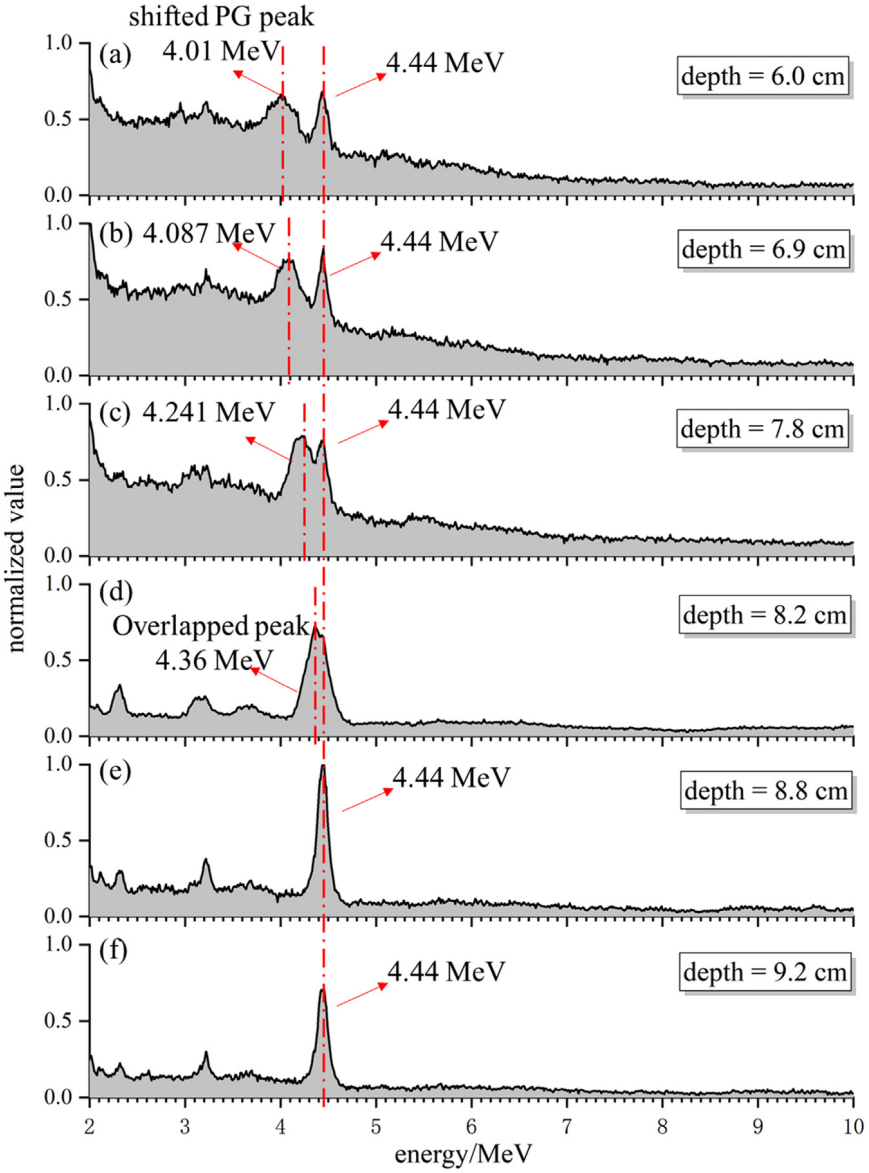

Fig. 3. PG ray spectra at depths of 6 cm (a), 6.9 cm (b), 7.8 cm (c), 8.2 cm (d), 8.8 cm (e), and 9.2 cm (f) in phase-space I with the emission direction respect to Z-axis restricted from 85 to 95 degrees.

polythene is less than 8.8 cm, which means little incident carbon ion exist at this depth. Fig. 4 also shows the PG spectra at depths of 6 cm, 7.8 cm and 8.8 cm in phase-space I without angle limitation. There are significant characteristic PG peaks with the energy of 4.44 MeV, but no shifted PG peak. That is because the shifted peak is different in different emission angle as predicted by the Formula 2 and when there is no angle limitation, multiple peaks overlap with each other which make the shifted peak not visible in the spectrum. The difference between Figs. 3 and 4 is the evidence proofing that the quantitative Doppler shift effect is influenced by the PG emission direction and the shifted PG peak can be visible in the spectrum only with collimator system (we also show the PG angle distribution in the supplemental material). Fig. 5 shows the PG spectra at depths of 6 cm, 7.8 cm and 8.8 cm in phase-space II with the emission direction respect to Z-axis restricted from 85 to 95 degrees. Similar to Fig. 3, there are 4.44 MeV and shifted PG peak in Fig. 5. Also, the energy of the shifted PG peak differs at different depths. The spectra detected in phase-space 1 and 2 with the similar condition show that the influence of the gamma attenuation and scattering is not evident in this case because of the high energy of the shifted PG energy. There are a lot of other characteristic peaks in Fig. 5, which seem to be shifted PG but the mechanism still uncertain.

3.2. PG energy shift distribution in the homogeneous phantom

To compare these two phase-space models quantificationally, we compared the shifted PG energy via analytical calculation and Monte Carlo simulation at different depths. The detail of the analytical method is explained in Section 2.2 and the shifted PG energies by the TOPAS simulation are quantified from the detected gamma spectra along the carbon beam path via Gaussian fitting. The quantitative comparison of the shifted PG energy with two phase-spaces is shown in Fig. 6. The results using phase-space I and II are similar because the high energy of these focused PG, which make the scattering effect in the phantom and air is not crucial in this simulation condition. For the case that near the entrance region of the carbon beam, the Monte Carlo results are in good agreement with the analytical calculation results. At the end of the range, the analytical method calculated values are generally smaller than those of the Monte Carlo simulation. This difference can be explained by several reasons. First, the analytical calculation does not reasonably consider the straggling of the beam energy, which has resulted in the broadening of carbon ion energy. As we only consider the average energy of carbon ion during the analytical calculation, the

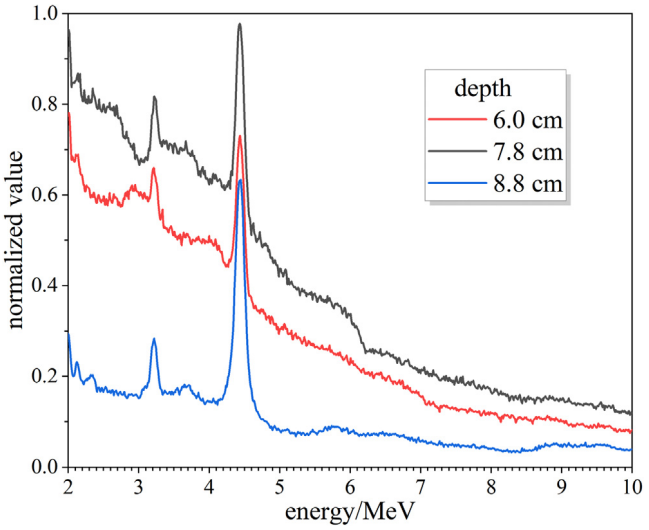

Fig. 4. PG ray spectra at depths of 6 cm, 7.8 cm and 8.8 cm in phase-space I without angle limitation (i.e., recording the particle whatever the value of its momentum).

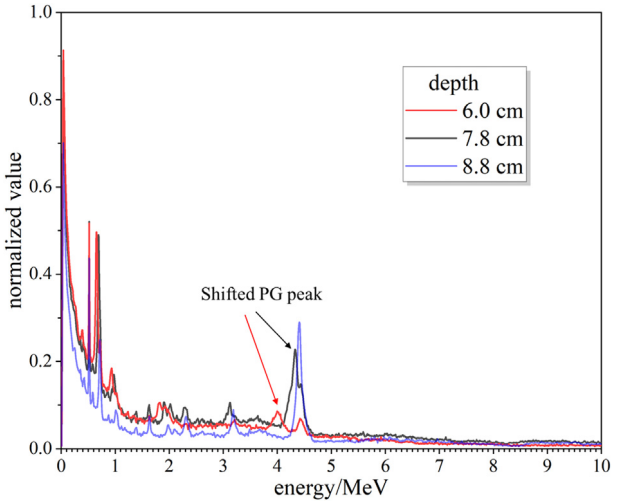

Fig. 5. PG spectra at depths of 6 cm, 7.8 cm and 8.8 cm in phase-space II with the detected direction respect to Z-axis restricted from 85 to 95 degrees.

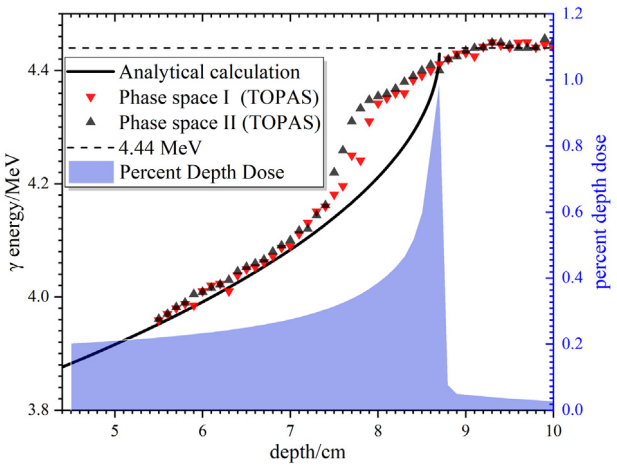

Fig. 6. Shifted PG energy at different depth using analytical calculation (solid line) and TOPAS simulation (red triangle for phase-space I and black triangle for phase-space II) when the phantom material is polyethylene.

shifted PG energy can be erroneous determined due to the different cross-section of gamma emission. Second, the shifted peak and the 4.44 MeV peak are too close to be accurately separated and quantified (e.g., Figs. 3c and 3d). In general, the Monte Carlo simulation results are consistent with the analytical calculation results, and the absolute difference value is approximately 0.868% (phase-space I) and 1.159% (phase-space II).

3.3. PG energy shift for different material configurations

The average difference values between the simulation results of the Monte Carlo method (phase-space I) and the analytical calculation with different phantom materials are shown in Table 1 and the average difference value for all regions is less than 1.2%. A moderate difference exists for the three groups of varying materials, except for the slightly higher difference value in the adipose phantom. As shown in Table 1, when we set the detection site from 5.5 cm to 7.5 cm, which represents a position where almost none of the peaks overlap in the spectrum, the difference value remarkably lower compared with the cases when the detection site is set from 7.5 cm to 9 cm, where severe peak overlap occurs in this group as shown in Fig. 3c and 3d. So, a suitable detection site needs to be considered with the prior information of patient geometry and beam energy. A relative shallow detection site allows for accurate energy detection. However, it may also lead to an extended residual region between the detection site and the carbon ion range, which means the uncertainty caused by the CT conversion factor in the residual region still exists. So, when choosing the detection site, these two influences should be considered and make a balance. Some mathematical methods in spectrum analyzing such as deconvolution and machine learning method can be used to eliminate the influence of peak overlap [26,27].

3.4. PG energy shift distribution in the CHRP

We further use the CHRP to study the performance with heterogeneity phantom using the proposed method. One carbon beam irradiates the abdomen and stops in the liver, and the other one irradiates the chest and stops in the lung. The results of both cases are shown in Fig. 7. As we can see in Fig. 7a, the distribution of the shifted gamma energy is very similar to the case that using the uniform phantom as the tissues along the beam path in the abdomen are semblable in the density and component. Comparing the results by Monte Carlo simulation and analytical calculation, they have almost the same trend along the beam path, and only near the range of the beam, Monte Carlo results are generally higher than the analytical results, as we have explained in Section 3.2. For the chest case, we can see that the shifted gamma distribution along the beam path is winding because the tissue of the lung are much lighter than the normal tissue, which makes the carbon beam loss its energy lower when crossing the lung. Also, the average difference value between Monte Carlo simulation and analytical calculation is less than 1%.

4. Summary

Carbon ion therapy has recently attracted considerable interest considering its superior dose distribution and high biological effectiveness. However, the issue of range uncertainty limits the full utilization of this therapy modality, thereby restricting the significance of the treatment outcome advantage. In this paper, we utilize the unique Doppler shift effect of prompt gamma for absolute range verification via spectroscopy and then reduce the safety margin. In order to apply this method in clinical in the future, we use Chinese hybrid radiation adult phantom (CHRP), a more complicated geometry model which could reproduce the characteristics of human body comparing to the much-simplified geometry model we used in the previous work, to verify the feasibility of the proposed method. Also, to reduce the calculation time, we

Table 1
Average difference values of analytical calculation and TOPAS simulation (phase-space I) in different phantom materials.

Difference value	5.5~7.5 cm (without peak overlap)	7.5~9 cm (with peak overlap)	All regions
Polyethylene	0.353%	1.511%	0.868%
Water	0.297%	1.558%	0.832%
Adipose	0.345%	2.050%	1.112%

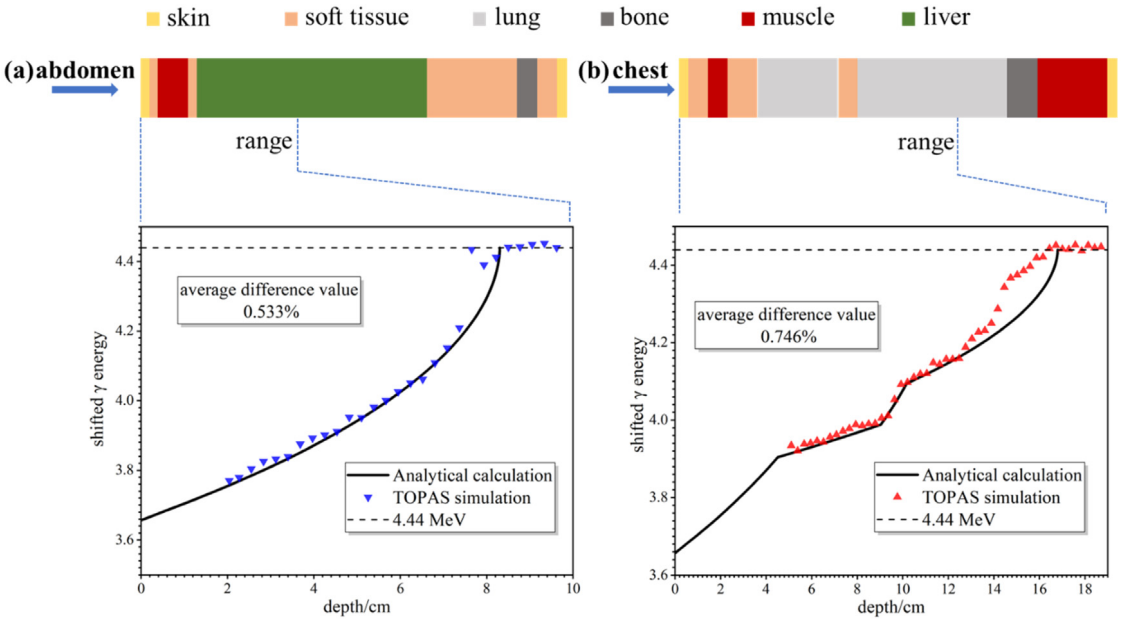

Fig. 7. The shifted gamma energy distribution along the beam path when the carbon beam irradiated the abdomen (a) and chest (b) using the CHRP.

discuss about the influence of two phase-spaces which are used to score particles. Its principle has been verified using the homogeneous phantom with different materials and CHRP as the distinct shifted PG peak with the energy less than 4.44 MeV appears on the spectrum. More importantly, the different PG energy shifts at different depths allow this method for range verification. The average difference values along the beam path between analytical calculation and Monte Carlo simulation are less than 2.1% in three different material phantoms, which prove the proposed method is not only limited to be used in the water phantom. Moreover, for the CHRP, the average difference value when irradiating chest is less than 0.8%, and when irradiating abdomen, that value is less than 0.6%, which could be a delightful result proving that the Doppler shift effect can be used in the human body with complicated material and geometry.

Considering the limitation of Monte Carlo simulation and analytical calculation at the current stage, we did not discuss some practical issues, such as scintillator inefficiency, energy resolution, temperature excursion and environmental noise, which may make it difficult to distinguish the shifted Prompt Gamma peaks [28]. Also, a stricter detector and analytical system are required to reduce the contribution of the escape peaks and the Compton edge. However, experiments to detect the accurate PG spectrum during the proton therapy for range verification shows that spectroscopy can be a promising way in carbon ion therapy. As this paper is preliminary research to show its possibility with different phantoms, details on applying this technique into a clinical scenario and complicated situations will be reported in the follow-up papers. Moreover, the proposed method is not limited in the field of radiotherapy. For situations in applied physics, where the carbon energy or range in the material needs to be known, this methodology can also be applied as an innovative tool.

Declaration of competing interest

The authors declare that they have no known competing financial interests or personal relationships that could have appeared to influence the work reported in this paper.

CRediT authorship contribution statement

Changran Geng: Methodology, Software, Validation, Writing - review & editing. **Yang Han:** Conceptualization, Formal analysis, Investigation, Writing - original draft, Data curation. **Xiaobin Tang:** Supervision, Project administration, Funding acquisition. **Diyun Shu:** Visualization. **Chunhui Gong:** Resources. **Saverio Altieri:** Writing - review & editing.

Acknowledgments

This work was supported by the National Natural Science Foundation of China (Grant No. 11805100 and 11905106); the National Key Research and Development Program (Grant No. 2016YFE0103600 and 2017YFC0107700); the Fundamental Research Funds for the Central Universities (Grant No. NS2018041); the Natural Science Foundation of Jiangsu Province (BK20180415); China Scholarship Council.

Appendix A. Supplementary data

Supplementary material related to this article can be found online at https://doi.org/10.1016/j.nima.2020.163439.

References

[1] J.S. Loeffler, M. Durante, Charged particle therapy—optimization, challenges and future directions, Nat. Rev. Clin. Oncol. 10 (2013) 411.

[2] D. Schardt, T. Elsässer, D. Schulz-Ertner, Heavy-ion tumor therapy: Physical and radiobiological benefits, Rev. Modern Phys. 82 (2010) 383.

[3] H. Ou, B. Zhang, S. Zhao, Monte Carlo simulation of the relative biological effectiveness and DNA damage from a 400 MeV/u carbon ion beam in water, Appl. Radiat. Isot. 136 (2018) 1–9.

[4] H. Paganetti, Range uncertainties in proton therapy and the role of Monte Carlo simulations, Phys. Med. Biol. 57 (2012) R99.

[5] H. Tsujii, T. Kamada, T. Shirai, K. Noda, H. Tsuji, K. Karasawa, Carbon-Ion Radiotherapy, Springer, 2014.

[6] A.-C. Knopf, A. Lomax, In vivo proton range verification: a review, Phys. Med. Biol. 58 (2013) R131.

[7] M. Moteabbed, S. España, H. Paganetti, Monte Carlo patient study on the comparison of prompt gamma and PET imaging for range verification in proton therapy, Phys. Med. Biol. 56 (2011) 1063.

[8] W. Enghardt, P. Crespo, F. Fiedler, R. Hinz, K. Parodi, J. Pawelke, F. Pönisch, Charged hadron tumour therapy monitoring by means of PET, Nucl. Instrum. Methods Phys. Res. A 525 (2004) 284–288.

[9] V. Ferrero, E. Fiorina, M. Morrocchi, F. Pennazio, G. Baroni, G. Battistoni, N. Belcari, M. Ciocca, A. Del Guerra, M. Donetti, Online proton therapy monitoring: clinical test of a silicon-photodetector-based in-beam PET, Sci. Rep. 8 (2018) 4100.

[10] I. Mattei, G. Battistoni, F. Bini, F. Collamati, E. De Lucia, M. Durante, R. Faccini, C. La Tessa, M. Marafini, L. Piersanti, Prompt-γ production of 220 MeV/u 12C ions interacting with a PMMA target, J. Instrum. 10 (2015) P10034.

[11] H.-M. Huang, M.-L. Jan, Accuracy of using high-energy prompt gamma to verify proton beam range with a compton camera: A Monte Carlo simulation study, Appl. Radiat. Isot. 142 (2018) 173–180.

[12] J. Krimmer, D. Dauvergne, J. Létang, É. Testa, Prompt-gamma monitoring in hadrontherapy: A review, Nucl. Instrum. Methods Phys. Res. A 878 (2018) 58–73.

[13] J.M. Verburg, J. Seco, Proton range verification through prompt gamma-ray spectroscopy, Phys. Med. Biol. 59 (2014) 7089.

[14] F. Hueso-González, M. Rabe, T.A. Ruggieri, T. Bortfeld, J.M. Verburg, A full-scale clinical prototype for proton range verification using prompt gamma-ray spectroscopy, Phys. Med. Biol. 63 (2018) 185019.

[15] S. Lehrack, W. Assmann, K. Parodi, Ionoacoustics for range monitoring of proton therapy, J. Phys. (2019) 012015.

[16] Y. Han, X. Tang, C. Geng, D. Shu, C. Gong, X. Zhang, S. Wu, X. Zhang, Investigation of in vivo beam range verification in carbon ion therapy using the Doppler shift effect of prompt gamma: A Monte Carlo simulation study, Radiat. Phys. Chem. 162 (2019) 72–81.

[17] Y.-S. Huang, K.-H. Lu, Formulation of the classical and the relativistic Doppler effect by a systematic method, Can. J. Phys. 82 (2004) 957–964.

[18] A.C. Kraan, Range verification methods in particle therapy: underlying physics and Monte Carlo modeling, Front. Oncol. 5 (2015) 150.

[19] J. Perl, J. Shin, J. Schümann, B. Faddegon, H. Paganetti, TOPAS: An innovative proton Monte Carlo platform for research and clinical applications, Med. Phys. 39 (2012) 6818–6837.

[20] J. Allison, K. Amako, J. Apostolakis, H. Araujo, P.A. Dubois, M. Asai, G. Barrand, R. Capra, S. Chauvie, R. Chytracek, Geant4 developments and applications, IEEE Trans. Nucl. Sci. 53 (2006) 270–278.

[21] J. Allison, K. Amako, J. Apostolakis, P. Arce, M. Asai, T. Aso, E. Bagli, A. Bagulya, S. Banerjee, G. Barrand, Recent developments in Geant4, Nucl. Instrum. Methods Phys. Res. A 835 (2016) 186–225.

[22] S. Agostinelli, J. Allison, K.a. Amako, J. Apostolakis, H. Araujo, P. Arce, M. Asai, D. Axen, S. Banerjee, G. Barrand, GEANT4—a simulation toolkit, Nucl. Instrum. Methods Phys. Res. A 506 (2003) 250–303.

[23] M. Zarifi, S. Guatelli, D. Bolst, B. Hutton, A. Rosenfeld, Y. Qi, Characterization of prompt gamma-ray emission with respect to the Bragg peak for proton beam range verification: A Monte Carlo study, Phys. Medica 33 (2017) 197–206.

[24] C. Geng, X. Tang, X. Hou, D. Shu, D. Chen, Development of Chinese hybrid radiation adult phantoms and their application to external dosimetry, Sci. China 57 (2014) 713–719.

[25] I.C.o.R, Units, Measurements, Photon, Electron, Proton and Neutron Interaction Data for Body Tissues, ICRU Report No. 46, 1992.

[26] A. Baeza, J. Miranda, J. Guillén, J. Corbacho, R. Pérez, A new approach to the analysis of alpha spectra based on neural network techniques, Nucl. Instrum. Methods Phys. Res. A 652 (2011) 450–453.

[27] H. Liu, M. Zhou, Z. Zhang, J. Shu, T. Liu, T. Zhang, Multi-order blind deconvolution algorithm with adaptive Tikhonov regularization for infrared spectroscopic data, Infrared Phys. Technol. 71 (2015) 63–69.

[28] L. Kelleter, A. Wrońska, J. Besuglow, A. Konefał, K. Laihem, J. Leidner, A. Magiera, K. Parodi, K. Rusiecka, A. Stahl, Spectroscopic study of prompt-gamma emission for range verification in proton therapy, Phys. Medica 34 (2017) 7–17.